# Coilin enhances phosphorylation and stability of DGCR8 and promotes miRNA biogenesis

Katheryn E. Lett, Madelyn K. Logan, Douglas M. McLaurin, and Michael D. Hebert*
Department of Cell and Molecular Biology, University of Mississippi Medical Center, Jackson, MS 39216-4505

**ABSTRACT** **MicroRNAs (miRNAs) are ~22 nt small noncoding RNAs that control gene expression at the posttranscriptional level through translational inhibition and destabilization of their target mRNAs. The biogenesis of miRNAs involves a series of processing steps beginning with cropping of the primary miRNA transcript by the Microprocessor complex, which is composed of Drosha and DGCR8. Here we report a novel regulatory interaction between the Microprocessor components and coilin, the Cajal body (CB) marker protein. Coilin knockdown causes alterations in the level of primary and mature miRNAs, let-7a and miR-34a, and their miRNA targets, HMGA2 and Notch1, respectively. We also found that coilin knockdown affects the levels of DGCR8 and Drosha in cells with (HeLa) and without (WI-38) CBs. To further explore the role of coilin in miRNA biogenesis, we conducted a series of coimmunoprecipitation experiments using coilin and DGCR8 constructs, which revealed that coilin and DGCR8 can form a complex. Additionally, our results indicate that phosphorylation of DGCR8, which has been shown to increase protein stability, is impacted by coilin knockdown. Collectively, our results implicate coilin as a member of the regulatory network governing miRNA biogenesis.**

**Monitoring Editor**
Anita Corbett
Emory University

Received: May 3, 2021
Revised: Jul 15, 2021
Accepted: Jul 20, 2021

## INTRODUCTION

Disruption of microRNA (miRNA) function is associated with many diseases (Lekka and Hall, 2018). The major components of the miRNA biogenesis pathway are Drosha, DGCR8, and Dicer (Bernstein *et al.*, 2001; Grishok *et al.*, 2001; Hutvagner *et al.*, 2001; Ketting *et al.*, 2001; Knight and Bass, 2001; Lee *et al.*, 2003; Denli *et al.*, 2004; Zeng *et al.*, 2005). Drosha and DGCR8 are the primary components of the Microprocessor, which plays a crucial role in the biogenesis of most animal miRNAs (Ha and Kim 2014; Treiber *et al.*, 2019). Specifically, in an activity known as cropping, DGCR8 directs the RNase III enzyme Drosha to process hairpins present in primary miRNA transcripts, yielding precursor miRNA (Han *et al.*, 2004; Partin *et al.*, 2017). Precursor miRNAs are then exported to the cytoplasm for additional biogenesis steps mediated by Dicer (Chendrimada *et al.*, 2005).

Numerous modulators influence the Microprocessor (Gregory *et al.*, 2004; Ha and Kim, 2014; Gurtner *et al.*, 2016; Michlewski and Caceres, 2019; Treiber *et al.*, 2019). Mechanisms have also been revealed that directly impact Drosha and DGCR8 function. For example, one very well-described pathway is the cross-regulation between Drosha and DGCR8 (Han *et al.*, 2009; Triboulet *et al.*, 2009). Specifically, hairpins present in the 5′ end of DGCR8 mRNA are cleaved by the Microprocessor, which reduces DGCR8 protein levels. In addition, Drosha is stabilized by DGCR8 interaction (Han *et al.*, 2009). Other regulatory mechanisms involve Drosha and DGCR8 post-translational modifications and interacting proteins (Tang *et al.*, 2010, 2011, 2013; Kawahara and Mieda-Sato, 2012; Wada *et al.*, 2012; Di Carlo *et al.*, 2013; Cheng *et al.*, 2014), such as the increased stability of DGCR8 by phosphorylation (Herbert *et al.*, 2013).

We previously identified a synergistic relationship between the Cajal body and the Microprocessor (Logan *et al.*, 2018, 2020; McLaurin *et al.*, 2020). Cajal bodies (CBs) are subnuclear domains that take part in the biogenesis of many different types of ribonucleoproteins (RNPs), including small nuclear RNPs (snRNPs) (Kiss 2004). The CB can be considered as an efficiency platform to generate sufficient RNP resources (Klingauf *et al.*, 2006; Morris

This article was published online ahead of print in MBoC in Press (http://www.molbiolcell.org/cgi/doi/10.1091/mbc.E21-05-0225).

*Address correspondence to: Michael D. Hebert (mhebert@umc.edu).

Abbreviations used: CB, cajal body; C19MC, chromosome 19 microRNA gene cluster; DAPI, 4′,6-diamidino-2-phenylindole; HMGA2, high mobility group AT-Hook 2; IF, immunofluorescence; IP, immunoprecipitation; KD, knockdown; miRNA, microRNA; RNP, ribonucleoproteins; scaRNA, small Cajal body-specific RNA; SMN, survival of motor neuron protein; snRNPs, small nuclear ribonucleoproteins; UT, untransfected.

2008) and is an invariant feature of transformed cell lines (Gall 2003). An important factor enriched in the CB is SMN, the survival of motor neuron protein. SMN is mutated in the neurodegenerative disease spinal muscular atrophy (Lefebvre *et al.,* 1995) and is important for snRNP formation (Lorson and Androphy 1998; Bertrandy *et al.,* 1999; Hebert *et al.,* 2001; Jones *et al.,* 2001; Pellizzoni *et al.,* 2001; Mahmoudi *et al.,* 2010; Broome and Hebert, 2012; Enwerem *et al.,* 2014; Machyna *et al.,* 2014; Poole *et al.,* 2016; Poole and Hebert, 2016). Reduced amounts of Drosha and dysregulated miRNA expression are observed in spinal muscular atrophy (Goncalves *et al.,* 2018). We observed that the Microprocessor contributes to the processing of certain small Cajal body–specific RNAs (scaRNAs; Tycowski *et al.,* 2004; Poole *et al.,* 2017; Burke *et al.,* 2018; Logan *et al.,* 2018, 2020; McLaurin *et al.,* 2020). In addition, we have found that CBs can associate with the chromosome 19 miRNA gene cluster (C19MC; Logan *et al.,* 2020). The C19MC region also recruits the Microprocessor, which provides a molecular link between CBs and Drosha/DGCR8 and suggests a novel role for CBs in the biogenesis of animal miRNAs. In support of this concept, we have reported that reduction of the CB marker protein coilin decreases the amount of a miRNA, miR-520 h, encoded by C19MC (Logan *et al.,* 2020). We also found that let-7a and its major target, HMGA2 (High Mobility Group AT-Hook 2) mRNA, are dysregulated upon coilin knockdown (KD; Logan *et al.,* 2020).

To more fully characterize the interrelationship between the Microprocessor and CBs, we evaluated candidate miRNA levels in both transformed and primary cell lines and found that coilin reduction disrupts miRNA biogenesis in all cells examined, including those that lack CBs. We also observed that coilin is part of a regulatory network with Drosha and DGCR8 and contributes to DGCR8 stability by promoting DGCR8 phosphorylation at S377. These data strongly indicate that nucleoplasmic coilin is a regulator for miRNA formation, and this regulation is not restricted only to cell types with CBs.

## RESULTS AND DISCUSSION

### Altered miRNA biogenesis in primary and transformed cells upon coilin reduction

To expand our understanding of CB-enriched proteins in miRNA processing and regulation of the Microprocessor, we evaluated primary miR-34a and mature miR-34a levels in both HeLa and WI-38 cells after 72 h coilin KD. Our previous studies demonstrate that snRNP resources are not greatly reduced with 72 h CB disruption (Logan *et al.,* 2020). MiR-34a was chosen as a candidate miRNA to examine because it is in encoded by an independently transcribed gene found in only one location in the human genome and, as part of the miR-34 family, is a well-studied tumor suppressor miRNA that inhibits fundamental signaling pathways such as Notch (Zhang *et al.,* 2019). The transformed HeLa cell line and the WI-38 primary cell vary in their nuclear organization, with CBs being abundant in HeLa but rare (present in 2–3% of cells) in WI-38 (Spector *et al.,* 1992). Hence studies using transformed and primary cell lines provide an opportunity to examine the nucleoplasmic role of CB-enriched proteins in the absence of CBs (Lam *et al.,* 2002). For our studies, we examined levels of primary and mature miRNAs, not precursor miRNAs. Drosha KD was conducted to serve as a positive control for the disruption of miRNA biogenesis in our analysis.

As shown in Figure 1A, Drosha KD in HeLa cells decreases mature miR-34a but increases primary miR-34a levels, consistent with a reduction in the cropping activity of the Microprocessor. This same trend (decreased mature and increased primary miR-34a) was also observed for coilin KD. Thus coilin KD is associated with the altered biogenesis of miRNAs encoded in large (miR-520 h) or small (let-7a) clusters (Logan *et al.,* 2020), as well as an independently transcribed miRNA gene present on one chromosome (miR-34a). Given that miR-34a is a known inhibitor of Notch (Zhang *et al.,* 2017; Zhang *et al.,* 2019), we also examined Notch mRNA levels after Drosha and coilin KD in HeLa cells and observed this mRNA was increased in both conditions (Figure 1B). To evaluate if cell types lacking CBs also show impaired miR-34a biogenesis upon coilin KD, we analyzed primary and mature miR-34a levels after 72 h coilin and Drosha KD in WI-38 cells. We observed that the reduction of both coilin and Drosha decreases mature miR-34a and increases primary miR-34a, although the increase of primary miR-34a is substantially higher with Drosha KD than with coilin (Figure 1C). The more drastic changes in primary and mature miRNAs in response to Drosha KD than with coilin KD are likely due to the fact that Drosha, being a part of the Microprocessor, is directly involved in processing primary miRNAs into precursor miRNAs, while coilin promotes miRNA biogenesis via an indirect mechanism. The reduction of mature miR-34a with both coilin and Drosha KD corresponded with an increase in Notch mRNA (Figure 1D). In addition to miR-34a, we also analyzed the level of primary and mature let-7a in WI-38 cells after 72 h coilin or Drosha KD and observed an increase in primary let-7a and a decrease in mature let-7a in both KD conditions (Figure 1E). We next investigated if the level of a major target mRNA for let-7a, HMGA2, is altered by coilin or Drosha reduction for 72 h in WI-38 cells. We found that both coilin and Drosha KD increase HMGA2 mRNA levels (Figure 1F). Collectively, these data support a role for coilin in the facilitation of miRNA biogenesis that is not limited to miRNAs encoded in clusters or cells that contain CBs.

### Coilin reduction in HeLa cells decreases DGCR8 protein levels

Previous work has shown that Microprocessor activity can be regulated by directly controlling Drosha and DGCR8 levels (Han *et al.,* 2009; Triboulet *et al.,* 2009). DGCR8 induction with Drosha KD is shown in Figure 2A (upper panel, lane 3) and quantified relative to β-actin protein in Figure 2B. Unexpectedly, we detected a small but statistically significant 25% decrease in DGCR8 protein levels upon coilin reduction compared with control siRNA treatment (Figure 2A, upper panel, lane 2, quantified in Figure 2B). In addition, the relative amount of coilin protein was found to be reduced upon Drosha KD (Figure 2A, quantified in Figure 2C). Drosha protein levels, however, were unaffected by coilin KD compared with that obtained with control siRNA (Figure 2A, quantified in Figure 2D). Likewise, relative SMN protein levels were unchanged with coilin or Drosha KD compared with control (Figure 2A).

To assess if the changes in protein levels shown in Figure 2A corresponded to altered mRNA levels, we conducted qRT-PCR to quantify the relative amount of DGCR8, coilin, and Drosha mRNA. As expected considering the cross-regulation between Drosha and DGCR8 (Han *et al.,* 2009; Triboulet *et al.,* 2009), the relative amount of DGCR8 mRNA was induced upon Drosha KD compared with that obtained with control siRNA (Figure 2E). Interestingly, we detected a small increase in DGCR8 mRNA upon coilin KD relative to control KD (Figure 2E), despite our observation that DGCR8 protein was slightly (25%) decreased in HeLa with coilin KD compared to control KD (Figure 2, A and B). These findings indicate that a posttranscriptional mechanism is responsible for the reduction of DGCR8 protein observed with coilin KD. Further analysis shows no change of coilin mRNA level with Drosha KD compared with control (Figure 2F) but an increase of Drosha mRNA with coilin KD (Figure 2G).

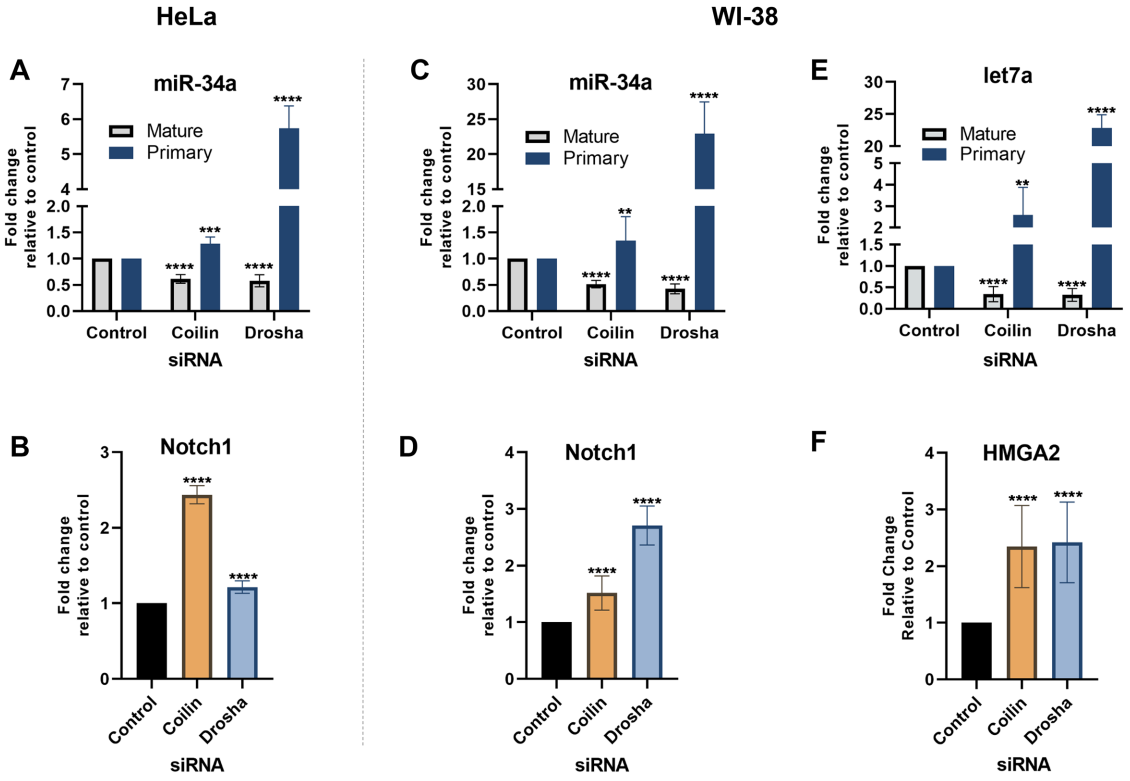


FIGURE 1: Coilin knockdown disrupts miRNA biogenesis. Quantitative PCR or RT-PCR was used to detect primary and mature miR-34a (A, C), primary and mature let-7a (E), Notch1 mRNA (B, D), and HMGA2 mRNA (F) in HeLa (A, B) and WI-38 (C–F) siRNA-transfected cells. The relative amount of a given amplicon in the control siRNA condition was set to 1. Data were derived from multiple biological (at least three) and technical (at least three) repeats, and error bars denote SD. ****$p < 0.0001$, ***$p < 0.0005$, **$p < 0.005$.

### Coilin is part of a regulatory network with Drosha and DGCR8

To more thoroughly examine a role for nucleoplasmic coilin in Microprocessor regulation, we treated WI-38 cells with various siRNAs. In agreement with previously published results (Han *et al.*, 2009; Triboulet *et al.*, 2009) and our findings in HeLa cells (Figure 2), Drosha reduction corresponded to an increase in DGCR8 protein (Figure 3A, upper panel, lane 2; Figure 3B). In contrast, coilin KD decreased DGCR8 protein levels in WI-38 cells (Figure 3A, upper panel, lane 3) as observed in HeLa cells (Figure 2A). However, we note that the reduction in DGCR8 protein upon coilin KD was more substantial in WI-38 (40%, Figure 3B) than in HeLa (25%, Figure 2B). A decrease in DGCR8 protein levels upon coilin KD was also observed in the IMR-90 primary cell line (Supplemental Figure 1). Additional analysis in WI-38 demonstrated that coilin protein was increased by Drosha KD (Figure 3, A and C) and Drosha protein was slightly increased by coilin KD (Figure 3, A and D). These findings were not observed in HeLa lysate (Figure 2). Relative SMN protein levels were unchanged with coilin or Drosha KD compared with control (Figure 3A) in WI-38 cells as they were in HeLa cells (Figure 2A).

We then examined DGCR8, coilin and Drosha mRNA levels in WI-38 cells following KD and found that Drosha and coilin KD induce DGCR8 mRNA (Figure 3E), similar to that observed in HeLa (Figure 2E). Also similar to that found in HeLa (Figure 2G), coilin KD increases Drosha mRNA in WI-38 (Figure 3G). Unlike in HeLa, however, Drosha KD in WI-38 cells increases coilin mRNA (Figure 3F). When considering the data from the transformed HeLa line and the primary WI-38 line, we find a consistent decrease in DGCR8 protein and increase in DGCR8 mRNA level upon coilin KD. A posttranscriptional mechanism could account for our observation that DGCR8 protein levels are decreased despite increased DGCR8 mRNA levels with coilin KD. The increase of coilin and Drosha protein in WI-38 with Drosha and coilin KD, respectively, may be indicative of transcriptional up-regulation or protein stability mechanisms and suggests that coilin and Drosha are negative regulators of each other.

### Coilin associates with the Microprocessor

To assess if coilin could be found in a complex with the Microprocessor, we conducted a series of coimmunoprecipitation (co-IP) experiments in HeLa cells with a variety of GFP-fused coilin constructs (Figure 4). We also utilized coilin constructs with GFP fused to the N-terminus or C-terminus of coilin (Figure 4A). In our previous work, we observed that GFP-coilin localized to the nucleoplasm and CBs like endogenous coilin, but coilin-GFP generated numerous CB-like foci with relatively less nucleoplasmic signal (Hebert and Matera, 2000; Shpargel *et al.*, 2003). Since the main components of the Microprocessor (Drosha and DGCR8) are nucleoplasmic and not enriched in mammalian CBs, we wanted to test if there was a difference in the amount of GFP-coilin versus coilin-GFP that associates with the Microprocessor. Lysate from untransfected (UT) HeLa cells or cotransfected with FLAG-DGCR8 plus myc-Drosha plasmids (Trans) was subject to IP with FLAG beads followed by SDS–PAGE, Western transfer, and detection of proteins with the indicated antibodies. Endogenous coilin is enriched by the FLAG-DGCR8/myc-Drosha Microprocessor complex from the amount of coilin recovered by FLAG beads using UT cell lysate (Figure 4B, upper; compare coilin signal in lane 4 with that in lane 3). In agreement with our previous publication (Burke *et al.*, 2019), we see an enrichment

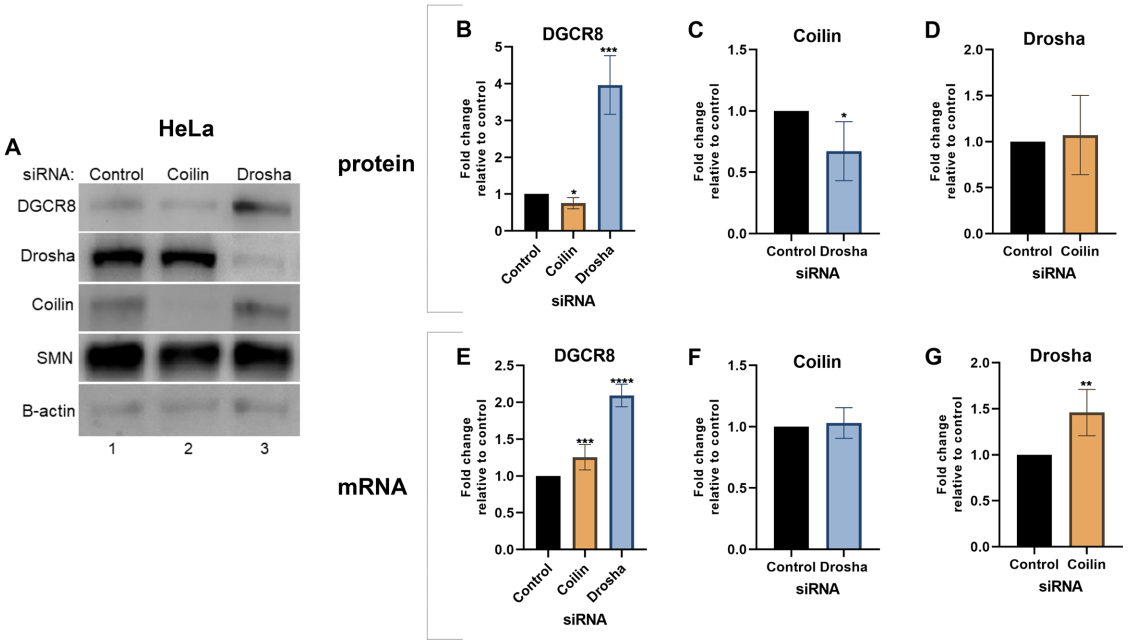


FIGURE 2: Coilin knockdown in HeLa decreases DGCR8 protein level. (A) DGCR8, Drosha, coilin, SMN, and β-actin protein as detected by Western blot with the indicated antibodies in HeLa siRNA treated cells. (B–D) Protein quantification of Western data was accomplished by normalizing to β-actin with the control siRNA ratio set to 1. $N = 5$ including three biological repeats. (E–G) mRNA quantification in HeLa KD cells with GAPDH mRNA as the normalizer. Data are shown with the negative control siRNA condition set to 1. $N = 9$, including three biological repeats. Error bars represent SD. * = $p < 0.05$, ** = $p < 0.005$, ***$p < 0.0005$, ****$p < 0.0001$.

of SMN recovered by the FLAG-DGCR8 IP beads compared with FLAG IP with UT lysate.

The amount of SMN and coilin found in the Microprocessor complex is not high when compared with the input signals, suggesting that these proteins are not an integral component of the Microprocessor but rather ancillary factors that may influence Microprocessor activity. To examine if other components enriched in the CB are also found in the Microprocessor complex, we tested for the presence of the WRAP53 protein (TCAB1/WDR79). WRAP53 is involved in the targeting of box H/ACA scaRNAs, including the telomerase RNA component, to the CB (Richard *et al.*, 2003; Tycowski *et al.*, 2009; Venteicher *et al.*, 2009). As shown in Figure 4B, lower panel, we do not detect a significant increase in the amount of endogenous WRAP53 signal present on the FLAG beads from cells cotransfected with FLAG-DGCR8/myc-Drosha (Trans) from that obtained with UT cells. These findings demonstrate that WRAP53 is not in a complex with Drosha/DGCR8, and indicate that not all proteins enriched in the CB form a complex with the Microprocessor.

We then evaluated the coilin constructs shown in Figure 4A for their ability to interact with FLAG-DGCR8. Cells were transfected with the indicated coilin construct alone or with FLAG-DGCR8 plasmid followed by IP with FLAG-beads. Both GFP-coilin and GFP-coilin (1-481) are enriched on FLAG-beads incubated with lysate expressing FLAG-DGCR8 (Figure 4C, right panel; compare the coilin signal in lane 2 with that in lane 1 and the coilin signal in lane 6 with that in lane 5). In contrast, we do not detect a signal above background for GFP-coilin (C214) or coilin-GFP. However, because both GFP-coilin (C214) and coilin-GFP were nonspecifically precipitated (Figure 4C, right panel, coilin signal in lanes 3 and 7), we cannot definitively conclude that there is no interaction between DGCR8 and GFP-coilin (C214) or coilin-GFP. To more definitely examine if GFP-coilin (C214) and coilin-GFP interact with the Microprocessor, a more stringent lysis and co-IP buffer will be utilized in future studies that decreases the amount of nonspecific binding of GFP-coilin (C214) and coilin-GFP to beads while maintaining association with the Microprocessor. Probing of this same blot with antibodies to Drosha demonstrates a tight interaction between FLAG-DGCR8 and endogenous Drosha. We then evaluated if FLAG-DGCR8 would co-IP with GFP-coilin (C214) or GFP-coilin (1-481) by cotransfecting these plasmids followed by IP with anti-GFP antibodies. As shown in Figure 4D, more DGCR8 is recovered by GFP-coilin (1-481) than by GFP-coilin (C214). Additionally, while the signal from DGCR8 recovered by GFP-coilin (C214) is not greater than that recovered by GFP antibodies from cells transfected with FLAG-DGCR8 alone (Supplementary Figure 1B; lane 3), this is not sufficient evidence to conclude that GFP-coilin (C214) does not interact with the Microprocessor. Co-IP data are summarized in Figure 4A. These results also indicate that the nucleoplasmic fraction of coilin interacts with the Microprocessor, in agreement with the lack of FLAG-DGCR8 enrichment in CBs or CB-like foci formed by the coilin constructs used here (Supplemental Figure 2). In other words, the Co-IP data are consistent with a model in which coilin and the Microprocessor interact in the nucleoplasm. However, our data do not eliminate the possibility that coilin/Microprocessor interactions could occur in CBs.

## Coilin promotes DGCR8 S377 phosphorylation and stability

The Microprocessor is regulated by many different mechanisms, some of which directly affect the central components of the Microprocessor, Drosha and DGCR8 (Gregory *et al.*, 2004; Han *et al.*, 2009; Triboulet *et al.*, 2009; Ha and Kim 2014; Gurtner *et al.*, 2016; Michlewski and Caceres 2019; Treiber *et al.*, 2019). Our results in HeLa, WI-38, and IMR-90 cell lines show that coilin appears to promote DGCR8 stability, considering that coilin KD decreases DGCR8

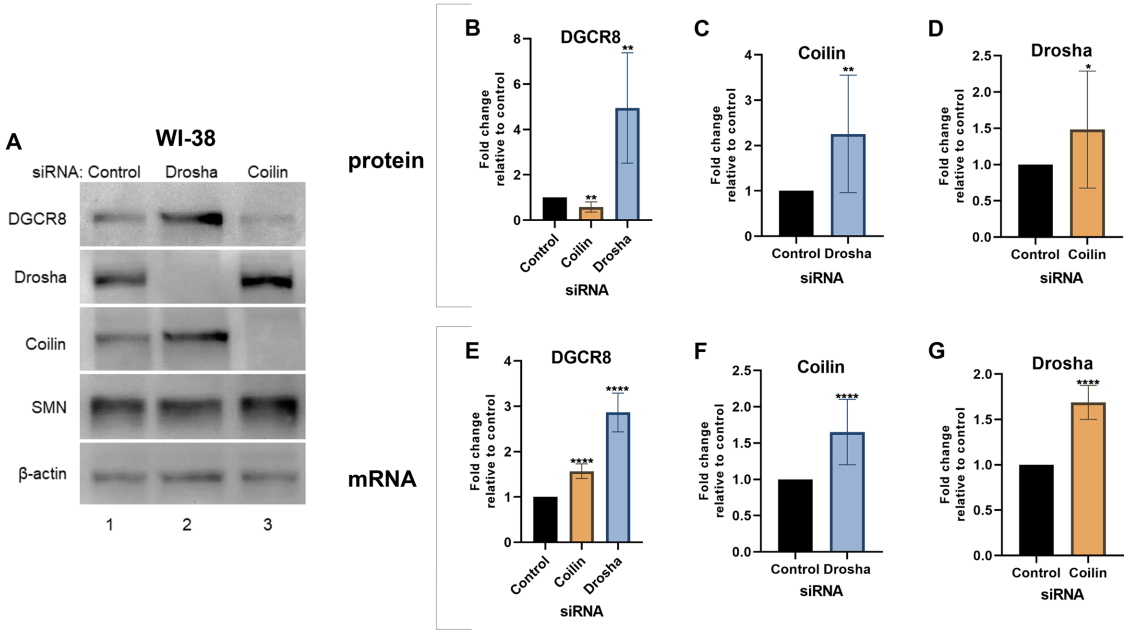


**FIGURE 3:** Coilin, DGCR8, and Drosha cross-regulation in WI-38 cells. (A) DGCR8, Drosha, coilin, SMN, and β-actin protein levels in WI-38 KD cells. (B–D) Protein quantification with signals normalized to β-actin and the negative control KD ratio set to 1. $N = 5$ including two biological repeats. (E–G) mRNA quantification in WI-38 KD cells with GAPDH as the normalizer and the negative control KD condition set to 1. $N = 9$, including three biological repeats. Error bars represent SD. * = $p < 0.05$, ** = $p < 0.005$, ****$p < 0.0001$.

protein level (Figures 2E and 3E). Two mechanisms shown to increase DGCR8 stability are phosphorylation (Herbert *et al.*, 2013) and SUMOylation (Zhu *et al.*, 2015). In regards to phosphorylation, 23 phosphorylation sites have been mapped in DGCR8, and increased DGCR8 phosphorylation is associated with increased protein stability, most likely due to the modification of DGCR8 by SUMO1 (small ubiquitin-like modifier 1), which prevents degradation by the ubiquitin proteasome pathway (Zhu *et al.*, 2015). To test if the observed reduced DGCR8 protein with coilin KD is a consequence of altered phosphorylation leading to decreased DGCR8 stability, we monitored the level of one known residue shown to be phosphorylated, S377 (Herbert *et al.*, 2013), as a proxy for the overall phosphorylation of DGCR8. For these experiments, WI-38 cells were transfected with control or coilin siRNA for 48 h and then transfected with FLAG-DGCR8 plasmid for 24 h, followed by IP using FLAG beads. The signal for phospho-DGCR8 (S377) is less in the IP reactions using coilin KD lysate than that obtained with control IP lysate (Figure 5A, upper panel; compare intensity of band in lane 4 with that in lane 3). This same blot was reprobed with antibodies to DGCR8 to obtain total DGCR8 levels. We then quantified the relative amount of phospho-DGCR8 (S377) signal for this and other experiments by dividing the phospho-DGCR8 (S377) signal by the total DGCR8 signal and normalizing to that obtained with control siRNA (Figure 5B). This analysis demonstrates that the phosphorylation of DGCR8 at S377 is decreased ~50% in coilin KD cells. Probing with antibodies to coilin show that the coilin siRNA is sufficient to reduce coilin protein (compare coilin signal in lane 2 to that in lane 1). Note that we did not detect endogenous coilin co-IP with FLAG-DGCR8 in these experiments, as we did in Figure 4, because we used a more stringent lysis buffer.

### A role for nucleoplasmic coilin in miRNA biogenesis

We show that coilin reduction disrupts miR-34a and let-7a miRNA biogenesis in cells lines with (HeLa) or without (WI-38) CBs (Figure 1). These findings indicate that coilin contributes to miRNA biogenesis in various contexts, including in CBs associated with large miRNA clusters like C19MC or in the nucleoplasm where it can facilitate the cropping of primary-miRNAs that are not encoded in large clusters, such as let-7a and miR-34a (Logan *et al.*, 2020). We have published that coilin KD for 5 d does not significantly decrease the splicing of mRNAs that encode miRNAs (Logan *et al.*, 2020). In WI-38 cells, however, proliferation assays show that coilin, Drosha, and SMN KD all have reduced proliferation rates at 3 d, so we conducted our analysis at 72 h rather than 120 h (Supplemental Figure 3).

Our data showing that DGCR8 is reduced and Drosha is increased upon coilin KD also provides more evidence for a role of coilin in miRNA biogenesis and establishes coilin as a regulator of the Microprocessor. Based on our IP data showing that coilin is associated with the Microprocessor complex, and our analysis showing that DGCR8 S377 phosphorylation is reduced upon coilin KD, we propose that coilin contributes to DGCR8 stability by promoting DGCR8 phosphorylation (Figure 5C). The mechanisms by which coilin inhibits accumulation of Drosha and Drosha inhibits accumulation of coilin await further investigation but may center upon transcriptional changes. Based on our experiments using transformed (HeLa) and primary cells (WI-38, IMR-90), these further investigations may be best conducted in primary cells as the observed dysregulations were most easily detected in primary cells. Our future studies also include investigations into the mechanism by which coilin facilitates DGCR8 phosphorylation, including an assessment of additional phosphorylation sites and an analysis as to if coilin impacts DGCR8 translation efficiencies. In summary, the work presented here provides evidence that coilin is a novel regulator of Microprocessor activity that complements the well-known regulatory network in which Drosha inhibits accumulation of DGCR8 and DGCR8 stabilizes Drosha (Figure 5C; Han *et al.*, 2009; Triboulet *et al.*, 2009).

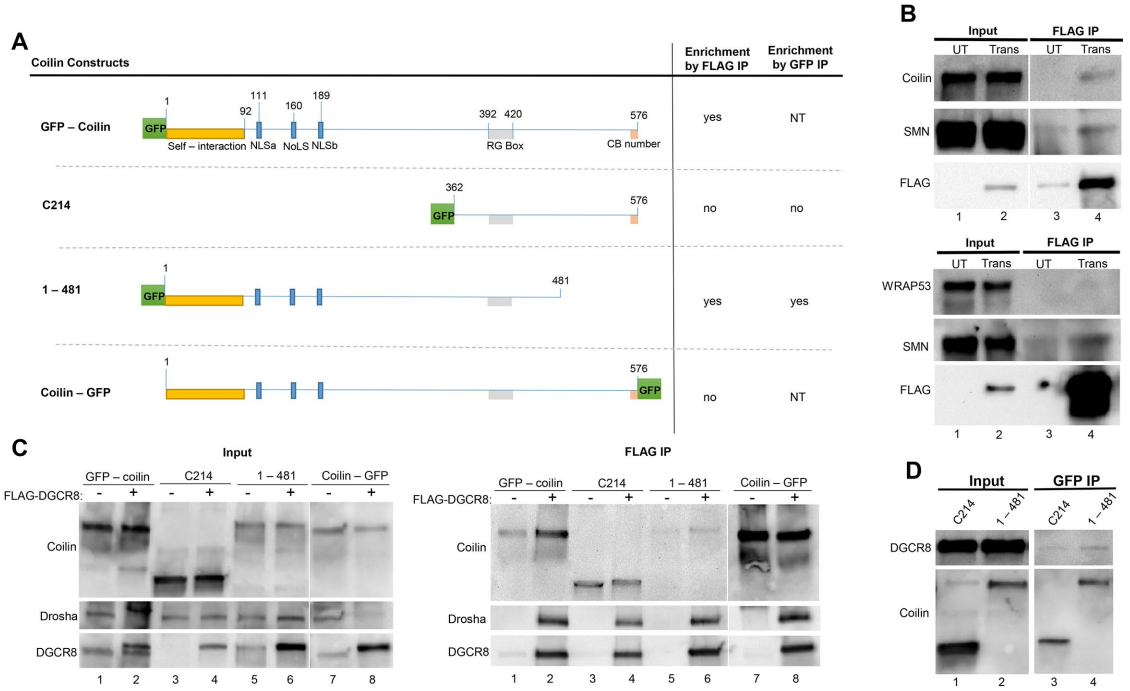


FIGURE 4: Coilin interacts with DGCR8 in HeLa. (A) Schematic of GFP-tagged coilin constructs. The self-interaction domain (yellow rectangle, Hebert and Matera, 2000), the nuclear and nucleolar localization signals (blue rectangles, Hebert and Matera 2000), the RG box (gray rectangle, Hebert *et al.*, 2002), and the C-terminal region that controls CB number (pink square, Shpargel *et al.*, 2003) are indicated. The right side summarizes the co-IP data shown in panels B–D. NT = not tested. DGCR8 IP using anti-FLAG beads (B and C) or anti-GFP antibodies coupled with protein G beads (D). In all experiments, input lanes account for 1.5% of the amount of lysate used in the IP reaction. (B) Lysate from untransfected (UT) or FLAG-DGCR8 plus myc-Drosha cotransfected (Trans) cells was subjected to IP with anti-FLAG beads, followed by Western detection using the indicted antibodies. (C) Cells were transfected with either coilin constructs alone (–, lanes 1, 3, 5, and 7) or both coilin constructs and FLAG-DGCR8 (+, lanes 2, 4, 6, and 8) for 24 h. Anti-FLAG beads were used to IP FLAG-DGCR8. Input lanes are shown in the left panel while IP reactions are shown in the right panel. The antibodies used to probe the membranes are indicated. (D) Cells were transfected with FLAG-DGCR8 and GFP-coilin (C214) or GFP-coilin (1–481) for 24 h. Anti-GFP was used to IP and the Western blot was probed with the indicated antibodies.

## MATERIALS AND METHODS

Request a protocol through *Bio-protocol*.

### Cell lines, plasmids, and transfections

HeLa (transformed) and WI-38 and IMR-90 (primary) cell lines were obtained from the American Type Culture Collection (ATCC). Cells were cultured as previously described (Enwerem *et al.*, 2014). All siRNAs were obtained from Integrated DNA Technologies (Coralville, IA) and utilized with RNAiMax (Invitrogen, Carlsbad, CA) per the manufacturer's protocol. Negative control, coilin 2, coilin A, coilin 3'UTR, SMN, and Drosha siRNAs were previously described (Poole and Hebert 2016; Logan *et al.*, 2018). All siRNA transfections were conducted for 72 h. DNA transfections in HeLa cells were conducted using FuGene HD (Promega, Madison, WI) according to the manufacturer's protocol. WI-38 DNA transfections were conducted using Lipofectamine 2000 (Invitrogen, Carlsbad, CA) per the manufacturer's protocol. GFP-coilin, coilin-GFP, and mutant coilin constructs: GFP-coilin 1-481 and GFP-coilin C214, plasmids have been previously described (Hebert *et al.*, 2002; Shpargel *et al.*, 2003). Myc-tagged Drosha and FLAG-tagged DGCR8 plasmids were obtained from Addgene (Watertown, MA). All DNA transfections were conducted for 24 h.

### Quantitative real-time PCR

RNA from HeLa and WI-38 cells was extracted with TRI-REAGENT (Molecular Research Center, Cincinnati, OH) according to the manufacturer's suggested protocol. Reactions were set up with 50 ng total RNA in Brilliant II SYBR Green qRT-PCR master mix (Agilent, Santa Clara, CA) using an Agilent MX3000P qRT-PCR system. Oligonucleotides used were obtained from Integrated DNA Technologies (Coralville, IA) with GAPDH, coilin, Drosha, primary let-7a, and HMGA2 as previously described (Burke *et al.*, 2019). Other primers used were Notch1: forward: (5'-GTGTGAAGCGGCCAATGGC-3'), reverse: (5'-GCTGGCACTCGTCCACATCC-3'); primary miR-34a: forward: (5'-GGGAGAGGCAGGACAGGCCTGTCC-3'), reverse: (5'-GCTTCATCTTCCCTCTTGGGCCCC-3'). For mRNA analysis, GAPDH served as the normalizer. The primers used for primary miR-34a and primary let7a do not overlap with the precursor miRNA sequences, so only the primary miRNAs were amplified. For RT-PCR detection of mature miRNAs, the miRCURY LNA (locked nucleic acid) RT and PCR kits (Qiagen, Germantown, MD) were used according to the manufacturer's protocol. Primers for 5s rRNA (which served as the normalizer), mature let-7a. and mature miR-34a were obtained from the manufacturer (Qiagen, Germantown, MD). Amplification rates, Ct values. and dissociation curve analyses of products were determined using MxPro (version 4.01) software. Relative expression was determined using the $2^{-\Delta\Delta CT}$ method (Livak and Schmittgen 2001). GraphPad Prism was used for post hoc statistical analysis using Student's *t* test and for histogram generation.

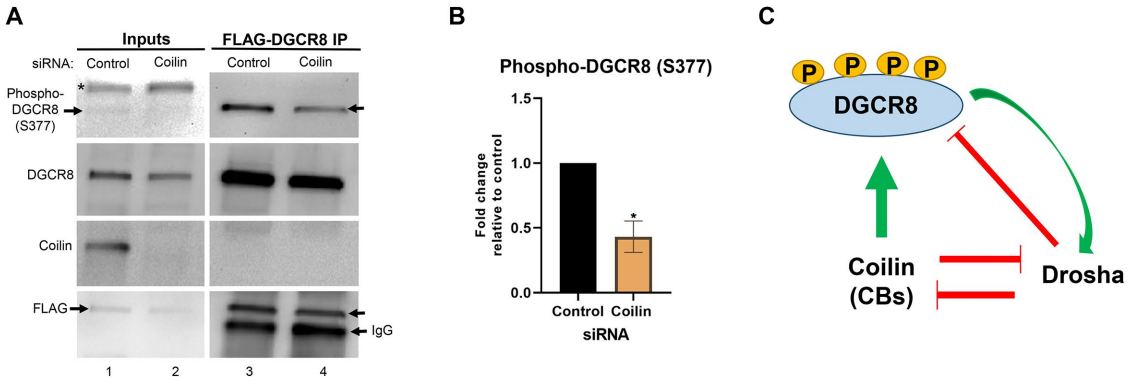


FIGURE 5: Coilin knockdown results in decreased phosphorylation of DGCR8 S377. (A) WI-38 cells were transfected with negative control or coilin siRNA, followed by transfection with FLAG-DGCR8. Anti-FLAG beads were used to IP FLAG-DGCR8 and the Western blot was probed with the indicated antibodies. * Nonspecific band detected by the phospho-DGCR8 (S377) antibody. (B) Quantification of phospho-DGCR8 (S377) signal relative to total DGCR8 signal in control and coilin knockdown. The ratio of phospho-DGCR8 (S377) signal to total DGCR8 signal in control siRNA reaction was set to 1. $N = 3$ biological. Error bars represent SD. *$p < 0.05$ (C) Model of the coilin, DGCR8, and Drosha regulatory network. Inhibitory (red) and promoting (green) actions are indicated.

### Immunofluorescence (IF)

HeLa cells were seeded on two-well glass slides. Once confluent, cells were cotransfected with FLAG-DGCR8 and either GFP-coilin, coilin-GFP, GFP-coilin 1-481, or GFP-coilin C214 constructs at a ratio of 1:3. For IF, cells were fixed in 4% paraformaldehyde within 5 min of retrieval from incubators followed by permeabilization in 0.5% Triton and blocked in 10% normal goat serum as previously described (Logan *et al.*, 2018). FLAG-DGCR8 was detected with 1:200 anti-FLAG mouse monoclonal antibody (F3165, Sigma Aldrich, St. Louis, MO) in 10% NGS at 37°C for 30 min. Slides were then washed with 1X PBS and incubated with 1:600 Alexa Fluor 594 (A32742, Invitrogen, Carlsbad, CA) goat anti-mouse (red) secondary antibody in 10% NGS at 37°C for 30 min. Slides were then washed in 1X PBS and 4′,6-diamidino-2-phenylindole (DAPI) stained to detect the nucleus followed by coverslip mounting with Antifade (Invitrogen, Carlsbad, CA). Cells were imaged as previously described (Poole *et al.*, 2016; Logan *et al.*, 2020).

### Immunoprecipitation (IP)

HeLa cells were cotransfected with FLAG-DGCR8 and myc-Drosha at a ratio of 1:4 or with FLAG-DGCR8 and a GFP-coilin construct at a ratio of 1:3 or with FLAG-DGCR8 alone for 24 h, and WI-38 cells were transfected with FLAG-DGCR8. After 24 h, WI-38 cells were lysed in RIPA buffer (50 mM Tris HCl pH 7.6, 150 mM NaCl, 1% NP-40, 0.25% Na-Deoxycholate, 1 mM EDTA, 0.1% SDS) plus protease inhibitor cocktail (Thermo Fisher Scientific) and HeLa cells were lysed in a modified RIPA buffer (50 mM Tris HCl pH 7.6, 150 mM NaCl, 1% NP-40, 0.25% Na-Deoxycholate, 1 mM EDTA, no SDS) plus protease inhibitor cocktail. All lysates were sonicated six times with a Fisher Scientific sonic dismembrator (Model 100) for 5 s each using the output setting of 1 and finally centrifuged at 12,000 rpm for 15 min at 4°C. WI-38 lysates and lysates from FLAG-DGCR8 and myc-Drosha cotransfected HeLa cells and untransfected controls were incubated with 40 µl anti-FLAG-M2 affinity agarose beads (Sigma Aldrich, St. Louis, MO) for 2 h. The GFP-coilin +/- FLAG-DGCR8 lysates were precleared using 60 µl protein G bead slurry followed by immunoprecipitation using 60 µl protein G beads and 2 µg anti-GFP mouse monoclonal antibody (sc-8334, Santa Cruz Biotechnology, Dallas, TX) or FLAG-DGCR8 immunoprecipitation using anti-FLAG-M2 affinity agarose beads (Sigma Aldrich, St. Louis, MO) for 2 h. HeLa and WI-38 immunoprecipitates were washed five times with modified RIPA buffer and RIPA buffer respectively, followed be analysis via Western blot.

### Western blotting

Cells were then lysed in RIPA as previously described (Poole and Hebert 2016) within 5 min of retrieval from the incubator. Lysate (15 µl) was run on a precast 10% Mini-Protean Gel (Bio-Rad Laboratories, Hercules, CA). For IP experiments described above, 20 µl of 2× SDS loading buffer was added to the beads. Immunoprecipitates and 15 µl of input lysates were run on a precast 10% Mini-Protean Gel (Bio-Rad Laboratories, Hercules, CA). Western transfer and detection were conducted as previously described (Poole and Hebert 2016). The primary antibodies used were anti-coilin rabbit polyclonal antibody (sc-32860, Santa Cruz Biotechnology, Dallas, TX); anti-Drosha rabbit monoclonal antibody (D28B1, Cell Signaling, Danvers, MA); anti-β-actin mouse monoclonal antibody (8H10D10, Cell Signaling, Danvers, MA); anti-SMN mouse monoclonal antibody (610646, BD Transduction Laboratories, San Jose, CA); anti-WRAP53 rabbit polyclonal antibody (A301-442A, Bethyl Laboratories, Montgomery, TX); anti-FLAG mouse monoclonal antibody (F3165, Sigma Aldrich, St. Louis, MO); anti-DGCR8 rabbit polyclonal antibody (ab90579, Abcam, Cambridge, MA); and anti-phospho-DGCR8 (Ser377) rabbit polyclonal antibody (PA5-35385, Invitrogen, Carlsbad, CA). Secondary antibodies used were goat anti-mouse HRP and goat anti-rabbit HRP. Bands were detected with SuperSignal West Pico Chemiluminescent Substrate (Thermo Scientific, Waltham, MA) following the manufacturer's suggested protocol. Imaging was done on a ChemiDoc (BioRad, Hercules, CA) with QuantityOne software. Adjustments to images were made using the transformation settings on QuantityOne software and applied across the entire image. Bands were quantified using QuantityOne software. GraphPad Prism was used for post-hoc statistical analysis using Student's *t* test and for histogram generation.

### Cell Proliferation Assay

WI-38 cells were seeded in a 24-well plate. Cells were transfected with negative control, coilin 2, coilin A, coilin 3′UTR, SMN, or Drosha siRNA. Cell viability was assessed using a CellTiter Blue Cell Viability Assay (G8081, Promega, Madison, WI). After 24, 48, and 72 h transfection, the CellTiter Blue reagent was added to the cells according to the manufacturer's suggested protocol and incubated for 1.5 h

and 3 h. Fluorescence was measured by a Biotek plate reader with Gen5 software. GraphPad Prism was used for post hoc statistical analysis using Student's *t* test and for histogram generation.


## ACKNOWLEDGMENTS

This work was supported by funds from the Department of Cell and Molecular Biology at the University of Mississippi Medical Center.


## REFERENCES


Bernstein E, Caudy AA, Hammond SM, Hannon GJ (2001). Role for a bidentate ribonuclease in the initiation step of RNA interference. Nature 409, 363–366.

Bertrandy S, Burlet P, Clermont O, Huber C, Fondrat C, Thierry-Mieg D, Munnich A, Lefebvre S (1999). The RNA-binding properties of SMN: deletion analysis of the zebrafish orthologue defines domains conserved in evolution. Hum Mol Genet 8, 775–782.

Broome HJ, Hebert MD (2012). In vitro RNase and nucleic acid binding activities implicate coilin in U snRNA processing. PLoS One 7, e36300.

Burke MF, Logan MK, Hebert MD (2018). Identification of additional regulatory RNPs that impact rRNA and U6 snRNA methylation. Biol Open 8, 30037971.

Burke MF, McLaurin DM, Logan MK, Hebert MD (2019). Alteration of 28S rRNA 2′-O-methylation by etoposide correlates with decreased SMN phosphorylation and reduced Drosha levels. Biol Open 8, 30858166.

Chendrimada TP, Gregory RI, Kumaraswamy E, Norman J, Cooch N, Nishikura K, Shiekhattar R (2005). TRBP recruits the Dicer complex to Ago2 for microRNA processing and gene silencing. Nature 436, 740–744.

Cheng TL, Wang Z, Liao Q, Zhu Y, Zhou WH, Xu W, Qiu Z (2014). MeCP2 suppresses nuclear microRNA processing and dendritic growth by regulating the DGCR8/Drosha complex. Dev Cell 28, 547–560.

Denli AM, Tops BB, Plasterk RH, Ketting RF, Hannon GJ (2004). Processing of primary microRNAs by the Microprocessor complex. Nature 432, 231–235.

Di Carlo V, Grossi E, Laneve P, Morlando M, Dini Modigliani S, Ballarino M, Bozzoni I, Caffarelli E (2013). TDP-43 regulates the microprocessor complex activity during in vitro neuronal differentiation. Mol Neurobiol 48, 952–963.

Enwerem, II, Velma V, Broome HJ, Kuna M, Begum RA, Hebert MD (2014). Coilin association with Box C/D scaRNA suggests a direct role for the Cajal body marker protein in scaRNP biogenesis. Biol Open 3, 240–249.

Gall JG (2003). The centennial of the Cajal body. Nat Rev Mol Cell Biol 4, 975–980.

Goncalves I, Brecht J, Thelen MP, Rehorst WA, Peters M, Lee HJ, Motameny S, Torres-Benito L, Ebrahimi-Fakhari D, Kononenko NL, *et al*. (2018). Neuronal activity regulates DROSHA via autophagy in spinal muscular atrophy. Sci Rep 8, 7907.

Gregory RI, Yan KP, Amuthan G, Chendrimada T, Doratotaj B, Cooch N, Shiekhattar R (2004). The Microprocessor complex mediates the genesis of microRNAs. Nature 432, 235–240.

Grishok A, Pasquinelli AE, Conte D, Li N, Parrish S, Ha I, Baillie DL, Fire A, Ruvkun G, Mello CC (2001). Genes and mechanisms related to RNA interference regulate expression of the small temporal RNAs that control *C. elegans* developmental timing. Cell 106, 23–34.

Gurtner A, Falcone E, Garibaldi F, Piaggio G (2016). Dysregulation of microRNA biogenesis in cancer: The impact of mutant p53 on Drosha complex activity. J Exp Clin Cancer Res 35, 45.

Ha M, Kim VN (2014). Regulation of microRNA biogenesis. Nat Rev Mol Cell Biol 15, 509–524.

Han J, Lee Y, Yeom KH, Kim YK, Jin H, Kim VN (2004). The Drosha–DGCR8 complex in primary microRNA processing. Genes Dev 18, 3016–3027.

Han J, Pedersen JS, Kwon SC, Belair CD, Kim YK, Yeom KH, Yang WY, Haussler D, Blelloch R, Kim VN (2009). Posttranscriptional crossregulation between Drosha and DGCR8. Cell 136, 75–84.

Hebert MD, Matera AG (2000). Self-association of coilin reveals a common theme in nuclear body localization. Mol Biol Cell 11, 4159–4171.

Hebert MD, Shpargel KB, Ospina JK, Tucker KE, Matera AG (2002). Coilin methylation regulates nuclear body formation. Dev Cell 3, 329–337.

Hebert MD, Szymczyk PW, Shpargel KB, Matera AG (2001). Coilin forms the bridge between Cajal bodies and SMN, the spinal muscular atrophy protein. Genes Dev 15, 2720–2729.

Herbert KM, Pimienta G, DeGregorio SJ, Alexandrov A, Steitz JA (2013). Phosphorylation of DGCR8 increases its intracellular stability and induces a progrowth miRNA profile. Cell Rep 5, 1070–1081.

Hutvagner G, McLachlan J, Pasquinelli AE, Balint E, Tuschl T, Zamore PD (2001). A cellular function for the RNA-interference enzyme Dicer in the maturation of the let-7 small temporal RNA. Science 293, 834–838.

Jones KW, Gorzynski K, Hales CM, Fischer U, Badbanchi F, Terns RM, Terns MP (2001). Direct interaction of the spinal muscular atrophy disease protein SMN with the small nucleolar RNA-associated protein fibrillarin. J Biol Chem 276, 38645–38651.

Kawahara Y, Mieda-Sato A (2012). TDP-43 promotes microRNA biogenesis as a component of the Drosha and Dicer complexes. Proc Natl Acad Sci USA 109, 3347–3352.

Ketting RF, Fischer SE, Bernstein E, Sijen T, Hannon GJ, Plasterk RH (2001). Dicer functions in RNA interference and in synthesis of small RNA involved in developmental timing in *C. elegans*. Genes Dev 15, 2654–2659.

Kiss T (2004). Biogenesis of small nuclear RNPs. J Cell Sci 117, 5949–5951.

Klingauf M, Stanek D, Neugebauer KM (2006). Enhancement of U4/U6 small nuclear ribonucleoprotein particle association in Cajal bodies predicted by mathematical modeling. Mol Biol Cell 17, 4972–4981.

Knight SW, Bass BL (2001). A role for the RNase III enzyme DCR-1 in RNA interference and germ line development in *Caenorhabditis elegans*. Science 293, 2269–2271.

Lam YW, Lyon CE, Lamond AI (2002). Large-scale isolation of Cajal bodies from HeLa cells. Mol Biol Cell 13, 2461–2473.

Lee Y, Ahn C, Han J, Choi H, Kim J, Yim J, Lee J, Provost P, Radmark O, Kim S, *et al*. (2003). The nuclear RNase III Drosha initiates microRNA processing. Nature 425, 415–419.

Lefebvre S, Burglen L, Reboullet S, Clermont O, Burlet P, Viollet L, Benichou B, Cruaud C, Millasseau P, Zeviani M, *et al*. (1995). Identification and characterization of a spinal muscular atrophy-determining gene. Cell 80, 155–165.

Lekka E, Hall J (2018). Noncoding RNAs in disease. FEBS Lett 592, 2884–2900.

Livak KJ, Schmittgen TD (2001). Analysis of relative gene expression data using real-time quantitative PCR and the 2(-Delta Delta C(T)) Method. Methods 25, 402–408.

Logan MK, Burke MF, Hebert MD (2018). Altered dynamics of scaRNA2 and scaRNA9 in response to stress correlates with disrupted nuclear organization. Biol Open 7, 30177550.

Logan MK, McLaurin DM, Hebert MD (2020). Synergistic interactions between Cajal bodies and the miRNA processing machinery. Mol Biol Cell mbcE20020144.

Lorson CL, Androphy EJ (1998). The domain encoded by exon 2 of the survival motor neuron protein mediates nucleic acid binding. Hum Mol Genet 7, 1269–1275.

Machyna M, Kehr S, Straube K, Kappei D, Buchholz F, Butter F, Ule J, Hertel J, Stadler PF, Neugebauer KM (2014). The coilin interactome identifies hundreds of small noncoding RNAs that traffic through Cajal bodies. Mol Cell 56, 389–399.

Mahmoudi S, Henriksson S, Weibrecht I, Smith S, Soderberg O, Stromblad S, Wiman KG, Farnebo M (2010). WRAP53 is essential for Cajal body formation and for targeting the survival of motor neuron complex to Cajal bodies. PLoS Biol 8, e1000521.

McLaurin DM, Logan MK, Lett KE, Hebert MD (2020). Molecular determinants that govern scaRNA processing by Drosha/DGCR8. Biol Open 10, 33037012.

Michlewski G, Caceres JF (2019). Post-transcriptional control of miRNA biogenesis. Rna 25, 1–16.

Morris GE (2008). The Cajal body. Biochim Biophys Acta 1783, 2108–2115.

Partin AC, Ngo TD, Herrell E, Jeong BC, Hon G, Nam Y (2017). Heme enables proper positioning of Drosha and DGCR8 on primary microRNAs. Nat Commun 8, 1737.

Pellizzoni L, Baccon J, Charroux B, Dreyfuss G (2001). The survival of motor neurons (SMN) protein interacts with the snoRNP proteins fibrillarin and GAR1. Curr Biol 11, 1079–1088.

Poole AR, Enwerem, II, Vicino IA, Coole JB, Smith SV, Hebert MD (2016). Identification of processing elements and interactors implicate SMN, coilin and the pseudogene-encoded coilp1 in telomerase and box C/D scaRNP biogenesis. RNA Biol 13, 955–972.

Poole AR, Hebert MD (2016). SMN and coilin negatively regulate dyskerin association with telomerase RNA. Biol Open 5, 27215323.

Poole AR, Vicino I, Adachi H, Yu YT, Hebert MD (2017). Regulatory RNPs: Aa novel class of ribonucleoproteins that potentially contribute to ribosome heterogeneity. Biol Open 6, 1342–1354.

Richard P, Darzacq X, Bertrand E, Jady BE, Verheggen C, Kiss T (2003). A common sequence motif determines the Cajal body-specific localization of box H/ACA scaRNAs. EMBO J 22, 4283–4293.

Shpargel KB, Ospina JK, Tucker KE, Matera AG, Hebert MD (2003). Control of Cajal body number is mediated by the coilin C-terminus. J Cell Sci 116, 303–312.
Spector DL, Lark G, Huang S (1992). Differences in snRNP localization between transformed and nontransformed cells. Mol Biol Cell 3, 555–569.
Tang X, Li M, Tucker L, Ramratnam B (2011). Glycogen synthase kinase 3 beta (GSK3beta) phosphorylates the RNAase III enzyme Drosha at S300 and S302. PLoS One 6, e20391.
Tang X, Wen S, Zheng D, Tucker L, Cao L, Pantazatos D, Moss SF, Ramratnam B (2013). Acetylation of drosha on the N-terminus inhibits its degradation by ubiquitination. PLoS One 8, e72503.
Tang X, Zhang Y, Tucker L, Ramratnam B (2010). Phosphorylation of the RNase III enzyme Drosha at Serine300 or Serine302 is required for its nuclear localization. Nucleic Acids Res 38, 6610–6619.
Treiber T, Treiber N, Meister G (2019). Regulation of microRNA biogenesis and its crosstalk with other cellular pathways. Nat Rev Mol Cell Biol 20, 5–20.
Triboulet R, Chang HM, Lapierre RJ, Gregory RI (2009). Post-transcriptional control of DGCR8 expression by the Microprocessor. RNA 15, 1005–1011.
Tycowski KT, Aab A, Steitz JA (2004). Guide RNAs with 5′ caps and novel box C/D snoRNA-like domains for modification of snRNAs in metazoa. Curr Biol 14, 1985–1995.
Tycowski KT, Shu MD, Kukoyi A, Steitz JA (2009). A conserved WD40 protein binds the Cajal body localization signal of scaRNP particles. Mol Cell 34, 47–57.
Venteicher AS, Abreu EB, Meng Z, McCann KE, Terns RM, Veenstra TD, Terns MP, Artandi SE (2009). A human telomerase holoenzyme protein required for Cajal body localization and telomere synthesis. Science 323, 644–648.
Wada T, Kikuchi J, Furukawa Y (2012). Histone deacetylase 1 enhances microRNA processing via deacetylation of DGCR8. EMBO Rep 13, 142–149.
Zeng Y, Yi R, Cullen BR (2005). Recognition and cleavage of primary microRNA precursors by the nuclear processing enzyme Drosha. EMBO J 24, 138–148.
Zhang L, Liao Y, Tang L (2019). MicroRNA-34 family: A potential tumor suppressor and therapeutic candidate in cancer. J Exp Clin Cancer Res 38, 53.
Zhang X, Ai F, Li X, Tian L, Wang X, Shen S, Liu F (2017). MicroRNA-34a suppresses colorectal cancer metastasis by regulating Notch signaling. Oncol Lett 14, 2325–2333.
Zhu C, Chen C, Huang J, Zhang H, Zhao X, Deng R, Dou J, Jin H, Chen R, Xu M, *et al.* (2015). SUMOylation at K707 of DGCR8 controls direct function of primary microRNA. Nucleic Acids Res 43, 7945–7960.